EXPERIMENTAL AND NUMERICAL ANALYSIS OF THE KNOCKING PHENOMENON IN A GDI ENGINE

M. Costa[(a)], U. Sorge[(b)], B. M. Vaglieco[(c)], P. Sementa[(d)],F. Catapano[(e)]

[(a), (b), (c), (d), (e)] CNR – Istituto Motori, Viale Marconi, 8 – 80125, Naples, ITALY

[(a)]m.costa@im.cnr.it, [(b)]u.sorge@im.cnr.it, [(c)]b.m.vaglieco@im.cnr.it, [(c)]p.sementa@im.cnr.it, [(e)]f.catapano@im.cnr.it

ABSTRACT

The in-cylinder auto-ignition process leading to knocking in a GDI (gasoline direct injection) engine equipped with a high-pressure injector is numerically simulated. The turbocharged engine, 4-stroke, 4-cylinder, is also experimentally characterized at the test bench under stoichiometric conditions by varying the time of spark advance so to promote the occurrence of the knocking phenomenon. This last is numerically investigated by resorting to the Shell model, that allows reproducing within the combustion chamber the chemical activity of the mixture at low temperature in the *end-gas zone*. The simultaneous use of an Extended Coherent Flamelet Model (ECFM) for the combustion initiated by the spark plug allows calculating the pressure cycle, as well as the amount of CO produced under each considered operating condition. The link between the knocking occurrence and the CO amount at the exhaust is analyzed, together with the role of an intermediate species of the Shell model in localizing both spatially and temporally the occurrence of an undesired auto-ignition.

Keywords: multidimensional engine model, GDI, knocking.

1. INTRODUCTION

The tendency to knocking in spark ignition engines is favorably affected by the direct injection of gasoline within the combustion chamber, due to the decrease of the charge temperature consequent the evaporation process (Alkidas, 2007). Despite many investigations, the knocking phenomenon, however, is still a crucial topic in the design and development also of GDI engines, with remaining uncertainties and unsolved questions.

The knocking phenomenon limits the performance and the efficiency of an engine, preventing to exceed certain values of the compression ratio and spark advance. Knocking is known to appear as a characteristic metallic noise involving power loss, vibration, and, under particularly severe conditions, damage of mechanical parts.

Modeling and previewing the knocking occurrence is a really complicated matter, since it implies the need to take into account tents of reactions including hundreds of chemical species to reproduce the detailed underlying chemical mechanisms in the mixture not yet reached by the flame front initiated by the spark plug.

The auto-ignition of the so-called in-cylinder *end-gas zone*, in fact, results from a set of pre-flame or low temperature reactions, which lead to the start of combustion without an external source, but through the formation of not stable products of partial oxidation (peroxides, aldehydes, hydroperoxides, etc..) and thermal energy release. When the energy of chemical exothermic reactions exceeds the amount of heat transferred by the reagent system to the external environment, the combustion occurs spontaneously. As a result, the mixture temperature increases, rapidly accelerating the subsequent oxidation reactions.

The complex kind of the pre-flame reactions, of chain type between highly reactive species, produced in a manner superior to the consumed ones by different propagation reactions, may be controlled through the introduction of small amount of additives in the base fuel, which hinder or enhance the formation of radicals acting as chain propagators (Leppard, 1991; Li *et al.*, 1994).

Aim of this paper is to provide a better understanding of how the knocking is initiated in a GDI spark ignition engine. To this purpose, a synergic experimental and numerical study is performed: high temporal resolution pressure measurements are realized on a high performance turbocharged engine, together with multidimensional simulation of the in-cylinder energy conversion process carried out through a properly developed 3D model. In particular, different spark advances are tested to reach different levels of knocking intensity. The Fast Fourier Transforms (FFT) of the measured cycles allows identifying the frequency range of knocking. The lacks of the experimental data consequent the local nature of the phenomenon under study are overwhelmed through the in-cylinder numerical simulation, that relies on the simultaneous use of a *flamelet* model for the combustion initiated by the spark and a reduced kinetic scheme reproducing the auto-ignition of the *end-gas* mixture. The kinetic scheme, namely the Shell model, assumes the low-temperature activity as occurring through 8 steps involving 3 main fictitious species (indeed group of chemical species), that allows reproducing the major

chemical events, as branching, propagation or linear termination.

The Shell model has been widely used in engine applications related to both Diesel and spark ignition engines (Sazhina *et al.*, 1999; Costa *et al.*, 2005). Although this model was developed more than thirty years ago, it is still used for computational fluid dynamics (CFD) applications, due to its simplicity combined with a generalized description of the kinetic mechanism of ignition, which has been proved as adequate to predict the main phenomena of interest in a variety of situations. Other kinetic mechanisms developed subsequently to the Shell, on the other hand, have a much higher number of reactions and species involved, which makes for their use being of little interest in complex computational domains (Griffiths *et al.*, 1994; Sahetchian *et al.*, 1995).

2. EXPERIMENTAL APPARATUS

The experimental apparatus of the present work includes the following modules: the spark ignition engine, an electrical dynamometer, the fuel injection line, the data acquisition and control units, the emission measurement system. The electrical dynamometer allows operating the engine under both motoring and firing conditions, hence detecting the in-cylinder pressure data and exploring the engine behaviour under stationary and simple dynamic conditions.

A spark ignition GDI, inline 4-cylinder, 4-stroke, displacement of 1750 cm3, turbocharged, high performance engine is considered. It has a wall guided injection system with a 6-hole nozzle located between the intake valves and oriented at 70° with respect to the cylinder axis. The engine is equipped with a variation valve timing (VVT) system in order to optimize the intake and exhaust valves lift under each specific regime of operation. The engine is not equipped with after-treatment devices. Further details are reported in Table 1.

Table 1: Characteristics of the engine under study.

Engine characteristics	
Unitary displacement [cm^3]	435.5
Bore [mm]	83
Stroke [mm]	80.5
Turbine	Exh. gas turbocharger
Max. boost pressure [bar]	2.5
Valve timing	Int. and Exh. VVT
Compression ratio	9.5:1
Max. power [kW]	147.1 @ 5000 rpm
Max. torque [Nm]	320.4 @ 1400 rpm

An optical shaft encoder is used to transmit the crank shaft position to the electronic control unit for the electronic control. The information is in digital pulses, the encoder has two outputs, the first is the Top Dead Center (TDC) index signal with a resolution of 1 pulse/revolution, and the second is the crank angle degree marker (CDM) 1pulse/0.2degree. The engine is 4-stroke and the encoder gives as output two TDC signals per engine cycle. In order to determine the right crank shaft position, one pulse is suppressed via the dedicated software.

A quartz pressure transducer is installed into the spark plug in order to measure the in-cylinder pressure with a sensitivity of 19 pC/bar and a natural frequency of 130 kHz. Thanks to its characteristics, a good resolution at high engine speed is obtained. The in-cylinder pressure, the rate of heat release and the related parameters are evaluated on an individual cycle basis and/or averaged on 400 cycles (Zhao and Ladommatos, 2001, Heywood, 1988).

All the tests presented in the paper are carried out at the engine speed of 1500 rpm and high load. The absolute intake air pressure depends on the variable geometry turbocharger and it remains constant around 1300 mbar. The intake air temperature is kept at 323 K. The start of spark (SOS) is initially fixed at 700° (20° before TDC, BTDC), which corresponds to the maximum brake torque (MBT) condition achievable in the absence of knocking. In order to induce this last, the spark advance is progressively increased by steps of 5° crank angle. Commercial gasoline with 92 octane number is used. The fuel injection always occurs directly in the combustion chamber at the pressure of 10 MPa. The Start Of Injection (SOI) is fixed at 520° (200° BTDC). The direct fuel injection strategy is able to affect the combustion process and the pollutants formation (Sementa *et al.*, 2012). The duration of injection is fixed as equal to 4700 μs, that allows realizing a stoichiometric equivalence ratio, as measured by a lambda sensor installed in the engine exhaust. All the measurements are performed under steady state conditions. Each engine point is stabilized for around 10 seconds before starting the acquisition of the optical data and of the pressure signal.

Figure 1 shows the in-cylinder pressure in three different situations. Figure 1a shows the normal combustion cycle, having the spark advance at 20° BTDC. Figure 1b and 1c represents pressure cycles collected at two different SOSs, each greater than 5° with respect to the previous one. In particular, Figure 1a reports the average over 300 consecutive cycles in the MBT condition, Figure 1b and 1c report the instantaneous pressure curves corresponding to the 150th cycle of 300 consecutive ones. In Figure 1b and 1c the pressure traces show the typical ripples of knock. Their intensity increases as the spark advance is increased. During the test, the temperature in the combustion chamber increases because of the thermal evolution typical of engines under knocking condition.

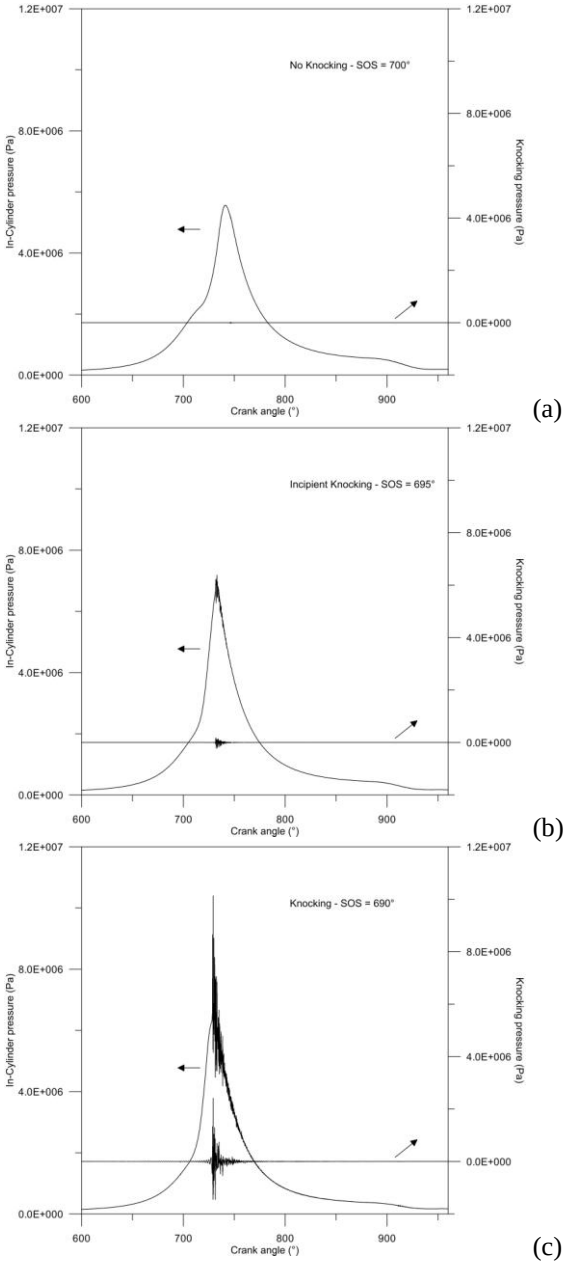

Figure 1: In-cylinder pressure in the no knocking, incipient knocking and knocking case and 5-30 kHz band pass filter.

To evaluate the knock signal, the 5 - 30 kHz band-pass filtering of the pressure signals is performed as also shown in Figure 1 (Draper, 1938; Checkel and Dale, 1989; Brunt *et al.*, 1998). The knock intensity is obtained by the peak-to-peak amplitude of the knock signal. The combustion cycles, therefore, are classified with respect to their knock intensity in the normal combustion, borderline knocking, (standard) knocking and heavy knocking cycle. If the knock intensity is lower than the 5% of the motored pressure at TDC, the engine works in normal combustion conditions. Until the 15%, a borderline knocking is considered. The standard knocking is associated to the range 15-20%. For knock pressures higher than the 20% of the motored pressure, the heavy knocking occurred (Mittal *et al*, 2007). According to this classification, the knock signals for the selected cycle reported in Figure 1c represents the heavy knocking. For this case, the knocking onset occurs after the combustion initiation by the spark plug and it continues for part of the expansion stroke.

For the selected cycles, the FFT shown in Figure 2 indicates that primarily two ranges of frequencies are excited, the range of the calculation only include the combustion phase from 20° BTDC at 50° ATDC. The lower frequency is around 5 kHz and it corresponds to the first circumferential frequency of the combustion chamber (Figure 3). Three different peak around these frequencies are well defined. A second range of frequencies is observed between 7 and 21 kHz without a single well-defined peak. This range of frequencies corresponds to the first axial mode due to the motion of the piston and to the second and higher circumferential modes. At increasing knock, an increase in amplitude for the lower and higher frequency is detected.

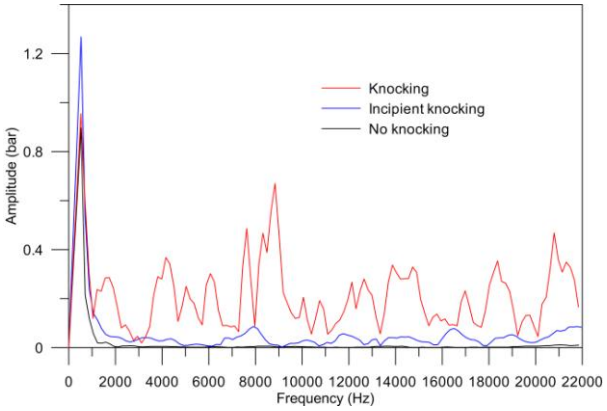

Figure 2: Pressure cycles Fast Fourier Transforms (FFT).

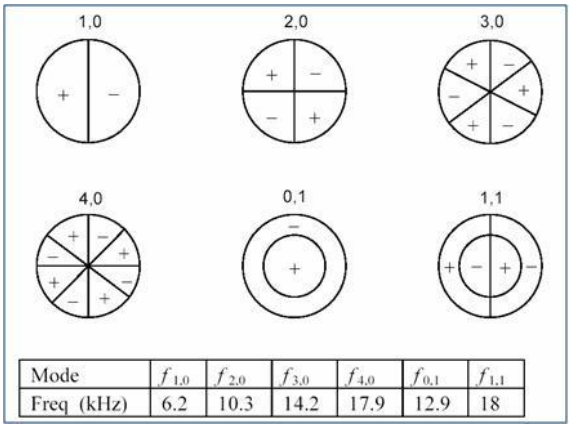

Figure 3: Frequency modes of cylinder vibration.

3. 3D ENGINE MODEL

The CFD 3D model for the engine under study is developed within the AVL Fire™ environment. The discretization of the computational domain

corresponding to the cylinder and the intake and exhaust ducts is made through the pre-processing module Fame Engine Plus (FEP), with part of the domain discretized "manually" to increase the mesh regularity and assure stability of computations. An idea of the mesh size is given by Table 2.

Table 2: Typical size of the employed meshes.

Grid size			
Range	Starting	Dead Center	Ending
Exhaust Stroke	413868	421788	287349
Intake Stroke	315080	336947	342839
Closed Valves	197951	159808	197951

The whole 4-stroke engine cycle is simulated. Boundary conditions for the 3D model are obtained from the test bench analysis. Mixture formation occurs through a six-hole injector manufactured by Magneti-Marelli, 0.140 mm of hole diameter and solenoid actuation, mounted between the two intake valves.

The delivered spray was preliminary experimentally characterized both at the mass flow rate test bench and in an optically accessible vessel. In a previous work, the collected data were used to develop a proper 3D model of the spray dynamics by Costa *et al.* (2012). The model considers the droplets break-up according to the Huh-Gosman model (Huh and Gosman, 1991), the effects on the droplets dynamics of the turbulent dispersion through the sub-model by O'Rouke (O'Rouke and Bracco 1980), the coalescence through the sub-model by Nordin (2001), the evaporation through the sub-model by Dukowicz (1979). In developing the 3D engine model here discussed, the spray model is modified to also account for the gasoline droplets impingement on the piston or cylinder walls. This is considered according to the model by Mundo-Sommerfeld (Mundo *et al.*, 1994).

Combustion is simulated through the Extended Coherent Flamelet Model (ECFM) (Colin, Benkenida, and Angelberger 2003), NO formation follows the Zeldovich's mechanism (Zeldovich *et* al., 1947). The ECFM model is properly tuned to well catch the in-cylinder pressure curve by acting on the initial flame surface density and the flame stretch factor. For the sake of brevity, further details of the validation procedure of the 3D model are here not reported. The interested reader may refer to the paper by Allocca *et al.* (2012). The comparison between the numerically computed in-cylinder pressure and the experimentally measured one in the normal combustion case of Figure 1a is shown in Figure 4. A good agreement is visible in the intake, compression, combustion and expansion phases. In particular, the start of combustion is well reproduced.

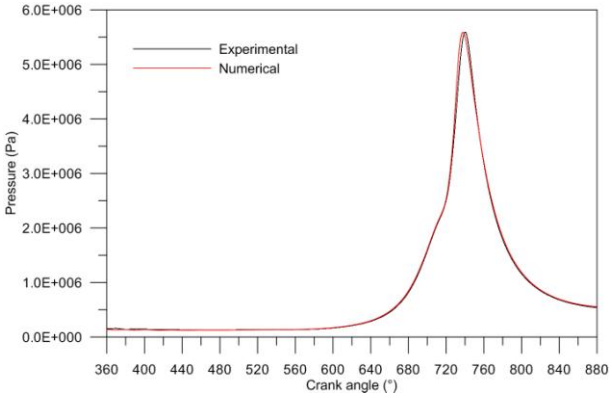

Figura 4: Experimentally measured and numerically computed in-cylinder pressure cycles.

The simulation of the auto-ignition process of an air-fuel mixture, as said within the introduction paragraph, can be carried out at different orders of approximation. A model that has proved successful in predicting both spatially and temporally the occurrence of the auto-ignition, and, at the same time, that does not require excessive computational time, is the so-called Shell model, developed by Halstead *et al.*, (1977). This model allows describing the process by schematization of the incubation phase of combustion through a reduced number of reactions involving not individual species, but groups of chemical compounds of similar behaviour.

Introducing the hydrocarbon RH, namely the fuel of composition C_xH_y, the Shell model is constituted by the following chemical reactions:

		kinetic costant
–	primary initialization	
	$RH + O_2 \rightarrow 2R*$	K_q
–	pre-flame propagation	
	$R* \rightarrow R* + P$	K_p
	$R* \rightarrow R* + B$	f_1K_p
	$R* \rightarrow R* + Q$	f_4K_p
	$R* + Q \rightarrow R* + B$	f_2K_p
–	branching	
	$B \rightarrow 2R*$	K_b
–	endings linear and quadratic	
	$R* \rightarrow NR$	f_3K_p
	$2R* \rightarrow NR$	K_t

where the letter P indicates the reaction products (CO_2, H_2O), while B and Q, respectively, represent branching agents and generic intermediate species. With the term NR are indicated not reacting compounds created at the end of the pre-flame reactions.

Into detail, the model contemplates the start of combustion, with the breaking of the chains of carbon-hydrogen fuel and the formation of radicals R*, and its development through the formation of oxygenated products. As already mentioned, the species that have a similar role in the kinetics of pre-flame are treated uniquely, as if they were a single entity. The advantages of using a reduced kinetic scheme, compared to a detailed scheme, consist just in the identification of groups of radicals or radicals which lead to branching of the chains of reaction or simple propagation of the linear type, and in the possibility to follow the variation in time of the concentration of these radicals.

The chemical pre-flame kinetics leading to the auto-ignition of the mixture not yet reached by the main flame front, within the present work, is reproduced after a proper tuning of the constants regulating the specific fuel reaction speed in the Shell model.

Some results of the 3D engine model are shown in Figures 5, 6 and 7 for the three conditions of Figure 1.

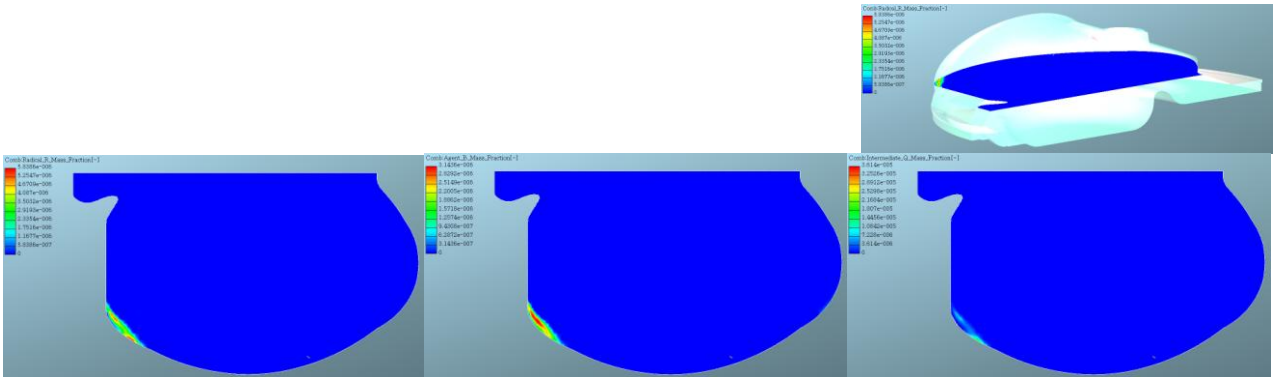

Figure 5: R* (left), B (middle) and Q (right) species on the plane orthogonal to the cylinder axis passing for the location of maximum Q for the no knocking case.

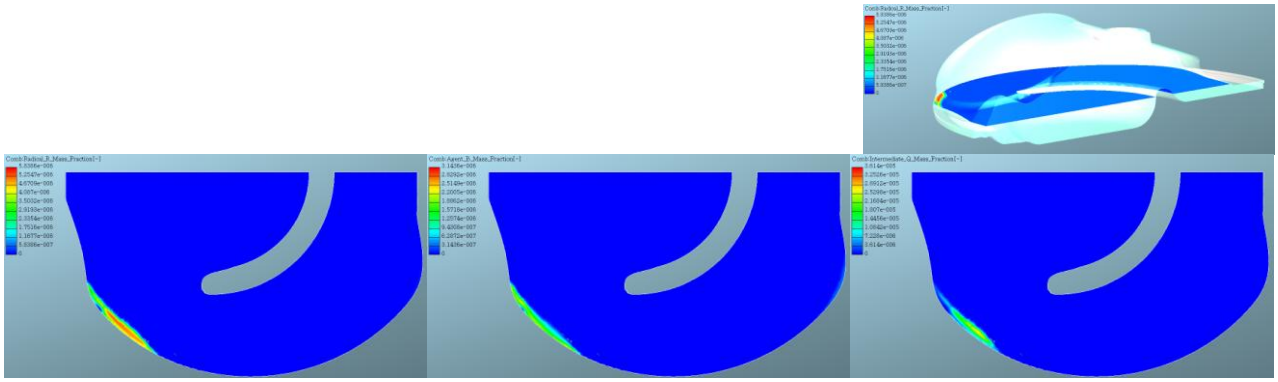

Figure 6: R* (left), B (middle) and Q (right) species on the plane orthogonal to the cylinder axis passing for the location of maximum Q for the borderline knocking cycle.

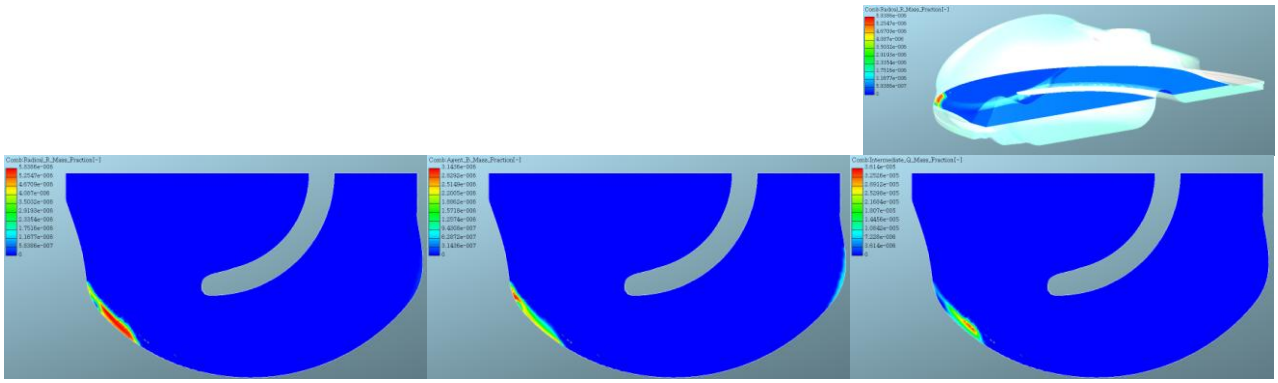

Figure 7: R* (left), B (middle) and Q (right) species on the plane orthogonal to the cylinder axis passing for the location of maximum Q for the heavy knocking cycle.

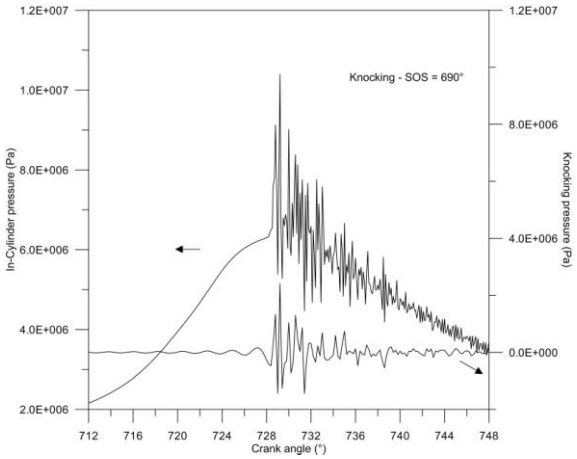

Figure 8. Particular of Figure 1C. Pressure cycle in the heavy knocking cycle.

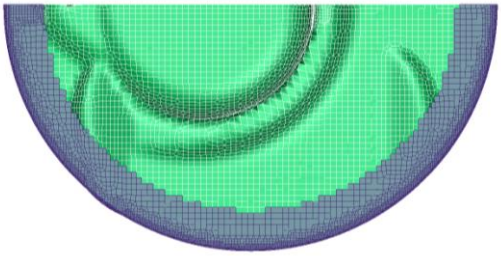
Figure 9: Piston surface and cells selection chosen to quantify the amount of formed Q species.

The R*, Q and B distributions in the combustion chamber are shown on planes orthogonal to the cylinder axis corresponding to the ones over which the species Q has its maximum value for each engine operation. This assures that the location where the most intense chemical activity is present is investigated for each engine operating condition defined by the specific value of SOS.

The crank angle considered for the case with SOS at 690°, is 729° (9 ° ATDC), that is in good agreement with the experimentally measured crank angle of knocking occurrence, as shown in Figure 8.

The chemical reactivity in the *end-gas zone* is higher in the knocking case, with a particularly high formation of the species Q, that may be taken as an indicator of the probability of knocking occurrence. From Figure 7, one may note that the most dangerous point for knocking onset within the combustion chamber is in the proximity of the wall on the intake valves and injector side, in agreement with the physical consideration that a decrease of the mixture temperature occurs in the opposite zone, where the spray is directed and mainly concentrated.

To better identify the variation of the Q species within the *end-gas zone*, a selection *ad hoc* is defined in the computational domain. In other words, the value of Q is calculated only in a volume made of the grid cells comprised within the annulus shown in Figure 9, having a thickness of 6 mm starting from the cylinder wall. As in Figures 5, 6 and 7, the intake valves and the injector are located on the left side, while the exhaust valves are on the right side.

In Figure 10 the mass fraction of the formed Q species in the afore mentioned cells selection is reported as a function of crank angle for the three different SOSs of Figure 1. The Q formation increases with increasing the spark advance, with the highest value occurring for SOS equal to 690°, thus confirming that the species Q is as a good knock indicator, identifying quite precisely the instant of crank angle where knocking occurs, as well as its location in space. The maximum of the Q relevant to the knocking case is just at 729°, namely at the knocking onset of Figure 8 (and 1.c). Figure 11 represents the maximum local value of the species Q mass fraction as a function of SOS, together with the angles measuring the interval of flame initiation and the flame propagation. These may be quantified by the interval of crank angle comprised between SOS and $\theta_{10\%}$ and the interval between $\theta_{10\%}$ and $\theta_{90\%}$, respectively. $\theta_{10\%}$ is the crank angle where the 10% of the mixture is burnt, while $\theta_{90\%}$ is the crank angle where the 90% of the mixture is burnt.

It is clear that by increasing the spark advance both the flame initiation and the flame propagation get slower. The greatest intervals needed for flame initiation and development at the highest spark advance, hence the unfavourable conditions of temperature and pressure at spark timing, give the mixture enough time to auto-ignite in the end-gas zone.

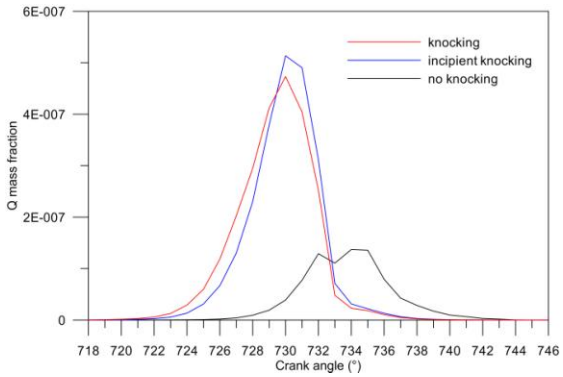

Figure 10: Trend of the species Q in the combustion chamber.

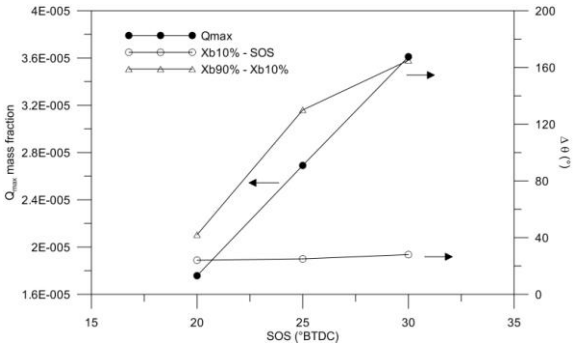

Figure 11: Maximum local value of species Q, flame initiation angle and flame development angle a function of SOS.

A good indicator of the mixture reactivity is also identified in the CO concentration at the exhaust valve opening, according to the paper by Li et al. (2007). As shown in Figure 12, the knocking case of Figure 1a exhibits a higher CO concentration at the exhaust valve opening with respect to cases of Figure 1b and 1c, having a 5° and 10° lower spark advance. This circumstance is also confirmed by Figure 13, where the numerically evaluated CO as a function of SOS are represented.

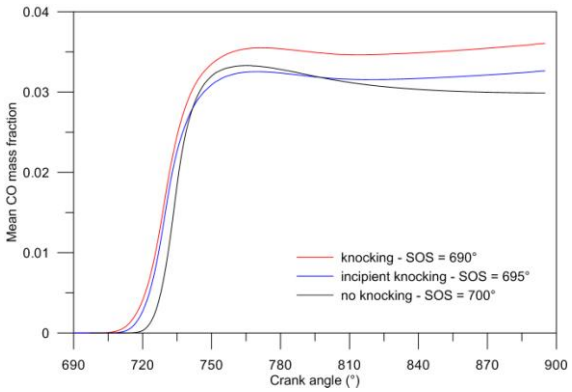

Figure 12: CO mass fraction computed by the 3D engine model in the combustion chamber.

4. CONCLUSION

A high performance GDI inline 4-cylinder, 4-stroke engine is experimentally tested under stoichiometric charge conditions to highlight the occurrence of knocking. The experimental measurements show that the increase of the spark advance increases the knocking intensity.

The knocking combustion is revealed through the FFT of the in-cylinder pressure that allows identifying the characteristic frequencies of the phenomenon.

Experimental data are employed to tune a properly developed 3D engine model, where the main combustion process is simulated through the ECFM model and the auto-ignition of the *end-gas zone* through the Shell model.

The computations show a good agreement with experiments as regards the knocking onset and its temporal location. The spatial position being the most probable for knocking is also highlighted. The chemical reactivity in the zone not yet reached by the flame front increases as the spark advance is increased, also as a consequence of the greatest time needed for flame initiation consequent the lower in-chamber value of temperature and pressure at spark timing.

The role of the species CO at exhaust valves opening, is shown as an indicator of the knocking occurrence. Indeed higher values are obtained in the case experimentally recognized as of heavy knocking.

REFERENCES

Alkidas, A.C., 2007. Combustion Advancements in Gasoline Engines, *Energy Conversion and Management*, 48, 2751-2761.

Allocca L., Costa M., Montanaro A., Sementa P., Sorge U., Vaglieco B.M., 2012. Characterization of the Mixture Formation Process in a GDI Engine Operating in Stratified Mode, *ICLASS 2012, 12th Triennial International Conference on Liquid Atomization and Spray Systems*, Heidelberg, (Germany), ISBN 978-88-903712-1-9.

Brunt, M.F., Pond, C.R., Biundo, J., 1998. Gasoline Engine Knock Analysis using Cylinder Pressure Data, *SAE Paper n. 980896*.

Checkel, M.D. and Dale, J.D., 1989. Pressure Trace Knock Measurements in a Current S.I. Production Engine. *SAE Paper n. 890243*.

Colin O., Benkenida A., Angelberger C., 2003. 3D Modeling of Mixing, Ignition and Combustion Phenomena in Highly Stratified Gasoline Engines, Oil & Gas Science and Technology – Rev. IFP Energies Nouvelles, 58, 47-62.

Costa M., Sorge U., Allocca L., 2012. CFD optimization for GDI spray model tuning and enhancement of engine performance, *Advances in Engineering Software*, 49, 43-53.

Costa M., Vaglieco B.M., Corcione F.E., 2005. Radical species participating the cool-flame regime of diesel combustion: a comparative numerical and experimental study, *Experiments in Fluids*, 39, 512-524.

Draper, C.S., 1938. Pressure Waves Accompanying Detonation in Internal Combustion Engine. *J. Aeronautical Sci*. Vol. 5.

Dukowicz J.K., 1979. Quasi-steady droplet change in the presence of convection, *informal report Los Alamos Scientific Laboratory*, Los Alamos Report LA7997-MS.

Griffiths, J.F., Hughes, K.J., Schreiber, M., Poppe, C., Dryer, F.L., 1994, A unified approach to the reduced kinetic modeling of alkane combustion, *Combustion and Flame*, 99 (3-4), 533-540.

Halstead, M.P., Kirsch, L.J., Quinn, C.P., 1977. The auto-ignition of hydrocarbon fuel at high temperatures and pressures – fitting of a mathematical model *Combustion and Flame*, 30, 45-60.

Heywood, J.B., 1988. *Internal Combustion Engine Fundamentals*, New York: McGraw-Hill.

Huh K.Y., Gosman A.D., 1991. A phenomenological model of diesel spray atomisation, *International Conference on Multiphase Flows*, Tsukuba, Japan.

Leppard, W.R., 1991. The autoignition chemistries of octane-enhancing ethers and cyclic ethers: A motored engine study, *SAE Paper 912313*.

Li, T., Nishida, K., Zhang, Y., Hiroyasu, H., 2007. Effect of split injection on stratified charge formation of direct injection spark ignition engines, *International Journal of Engine Research*, 8, 205-219.

Li, H., Prabhu, S., Miller, D., Cernansky, N., 1994. Autoignition Chemistry Studies on Primary Reference Fuels in a Motored Engine, *SAE Technical Paper 942062*.

Merola S.S, Sementa P., Tornatore C., Vaglieco B.M., 2009. Knocking Diagnostics in the Combustion Chamber of Boosted PFI SI Optical Engine. *International Journal of Vehicle Design*, Inderscience Publishers ed., 49, 70-90.

Mittal, V., Revier, B.M., Heywood, J.B., 2007. Phenomena that Determine Knock Onset in Spark-Ignition Engines, *SAE Paper n. 2007-01-0007*.

Mundo C., Sommerfeld M., Tropea M.C., 1994., Experimental Studies of the Deposition and Splashing of Small Liquid Droplets Impinging on a Flat Surface, *ICLASS-94 Rouen*, France.

Nordin W.H., 2001. *Complex Modeling of Diesel Spray Combustion*, Thesis (PhD), Chalmers University of Technology.

O'Rourke P.J., Bracco F.V., 1980. Modeling of Drop Interactions in Thick Sprays and a Comparison with Experiments, *Institution of Mechanical Engineers (IMECHE)*, London.

Sahetchian, K., Champoussin, J.C., Brun, M., Levy, N., Blin-Simiand, N., Aligrot, C., Jorand, F., Guerassi, N., 1995. Experimental study and modeling of dodecane ignition in a diesel engine, *Combustion and Flame*, 103 (3), 207-220.

Sazhina, E.M., Sazhin, S.S., Heikal, M.R., Marooney, C.J., 1999. The Shell Autoignition Model: Applications to Gasoline and Diesel Fuels, *Fuel*, 78, 389-401.

Sementa P., Vaglieco B.M., Catapano F., 2012. Thermodynamic and optical characterizations of a high performance GDI engine operating in homogeneous and stratified charge mixture conditions fueled with gasoline and bio-ethanol. *Fuel*, 96, 204-219.

Zeldovich Y.B., Sadovnikov P.Y., Frank-Kamenetskii D.A., 1947. Oxidation of Nitrogen in Combustion, *Translation by M. Shelef, Academy of Sciences of USSR, Institute of Chemical Physics*, Moscow-Leningrad.

Zhao, H., Ladommatos, N., 2001. *Engine Combustion Instrumentation and Diagnostics*, SAE Int., Inc.